The effect of partial substitution of Bi on colour properties and thermal stability of $Bi_xPr_{1-x}FeO_3$ pigments

Jana Luxová[1], Petra Šulcová[1]

Department of Inorganic Technology, Faculty of Chemical Technology, University of Pardubice, Doubravice 41, 532 10 Pardubice, Czech Republic, e-mail: jana.luxova@upce.cz

Abstract

The samples of $Bi_xPr_{1-x}FeO_3$ (x=0-0.3) were prepared by conventional ceramic method. The main aim of this work was to focus on determination of influence of partial Bi substitution for Pr on chromaticity and thermal stability. The formation temperature of the orthoferrites was chosen according to the results of DTA/TG analysis. X-ray powder diffraction analysis showed that solid solutions with orthorhombic structure were created. Results of the work proved that Bi substitution for Pr in $PrFeO_3$ has significantly impact on colour properties and thermal stability. Start of sintering of $PrFeO_3$ was detected at 1086 °C and due to substitution of Bi^{3+} decreased to 956 °C (for x = 0.3). Thermal stability of the samples with x = 0.2 and x = 0.3 was limited at 1371 °C, 1360 °C respectively. However, final colour was positively affected by the addition of Bi^{3+}. Colour shades of powders shifted from yellowish brown to reddish brown with increasing amount of Bi ions. Very interesting colours of different deep yellowish and reddish brown shades were obtained after their application into organic binder. Mean particle size for all milled compounds prepared at 1000 °C was around 1 μm and for samples calcined at 1100 °C ranged between 1 – 1.6 μm.

Keywords: Orthoferrite; Thermal analysis; Thermal stability; Optical properties

Introduction

At the present time, great emphasis is on environmental protection and utilization of environmentally friendly materials. Based on these facts, some materials have been identified as hazardous or toxic. The inorganic pigments were also affected by this ecological problem when the compounds contain toxic elements, especially Cr^{VI} and Pb were forbidden [1]. The search for new compounds and the design of new combinations with the aim of improving the properties of the existing materials are, hence, still a topical subject matter. One of the promising options could be perovskite compounds.

Oxide perovskite compounds have a general formula ABO_3 and they are derived from a naturally occurring mineral, calcium titanate. In this compound, A is formed by a large cation, while a smaller one is placed on B side. Oxide perovskites have a stoichiometry with a structure that consists a three-dimensional framework of corner-sharing BO_6 octahedron that contains A cations at 12-coordinate sites [2,3]. Amongst the perovskite compounds, there are the A^{3+}- B^{3+} or (3-3) perovskites, in their orthorhombic forms; the displacement of different A^{3+} cations from

ideal position appears to decrease with increasing the size of A^{3+} with the same B^{3+} cation. [2,4]. When Fe^{3+} ions are on the place B, the compounds are called orthoferrites [5].

Orthoferrites with the rare earth elements are attractive materials thanks to wide possibilities of their utilization. These compounds can be use as electronic materials [2], for development of solid-oxide fuel cells [6], chemical sensors for detection of humidity [2,7], alcohol [2,8] or some gases, like CO [9], NO_2 [10] or O_2 [11]. From other technological applications, it is possible to mention their use in development of oxygen permeation membranes [12] and oxygen sensor electrodes [13,14], as catalysts for methane combustion [15] or for the removal of gas pollutants by oxidation CO, reduction and decomposition of NO [16].

Interest about Ln doped orthoferrites also consists in the possibility to research and to investigate these compounds as inorganic pigments. Dopants based on rare earth elements in mixed oxides offer an opportunity to tune the colour response through manipulation of energy and delocalization phenomenon in conduction and valence bands, which can affect the optical properties of materials [17]. Resulted colours of the orthoferrites are very dependent not only on condition of the preparation [3], but also on the used Fe^{3+} precursors and rare earth oxides [18]. Generally, the pigments prepared from Fe_2O_3 were brighter and deeper, but on the other hand, compounds prepared from FeOOH contain bigger amount of the red hue. Based on determination of colour properties of $LnFeO_3$ (when Ln=La, Gd, Yb, Tm and Lu), the pigments can be divided into two groups: the first one is represented by pigments with the bigger ionic radius (La^{3+} and Gd^{3+}), which forms pigments with sienna colour; second group includes orthoferrites with smaller ionic radius (Tm^{3+}, Lu^{3+} and Yb^{3+}) forming compounds with reddish brown colours [18].

The attractiveness of the orthoferrite research also lies in an investigation of these compounds as multiferroic materials. The bismuth ferrite oxide belongs to the most studied multiferroics. Because it is the only material known to exhibit magnetic and ferroelectric order at room temperature [19]. $BiFeO_3$ is distinguished by its extremely high magnetic and ferromagnetic transition temperatures; it has rhombohedrally distorted structure and possesses a large polarization [20,21].

As mentioned above, $BiFeO_3$ is the one of the most studied multiferroic materials, primarily due to its high magnetic and electric transition temperatures: ferroelectric Curie temperature $T_C \approx$ 810-830 °C [22, 23] and antiferromagnetic temperature $T_N \approx$ 350-370 °C [23-25]. The phase diagram of Bi_2O_3-Fe_2O_3 system has been reported in the work of Palai et al. [26]. According to this work, existence of three distinct solid phases of $BiFeO_3$ was suggested. They observed α-β structural phase transition at around 820 °C and β-$BiFeO_3$ phase between 820-925 °C. Moreover, existence of a cubic γ-$BiFeO_3$ has been established between 925-933 °C. These results are consistent with the work of Alnold et al., where they demonstrated that $BiFeO_3$ undergoes the ferroelectric transition at T_C (820-830 °C) from the rhombohedral α-phase (R3c space group) to an orthorhombic β-phase (Pbnm space group) [27]. Rietveld study at 820 °C presented in this work shows a phase mixture of ~93% α-$BiFeO_3$, 3% β-$BiFeO_3$ and 3% $Bi_2Fe_4O_9$ and at 825 °C, the phase fractions are 12% α, 82% β and 6%, respectively. The β-

phase of $BiFeO_3$ persists up to a temperature of approximately 890 °C [27]. The third solid phase of $BiFeO_3$ has been marked as the γ-phase, and it persists up to temperatures of approximately 955 °C [25].

Synthesis of single-phase bismuth ferrite prepared by solid state reaction can be very difficult. For the preparation of pure $BiFeO_3$ from oxides, ultrapure starting oxides are necessary to used. When $BiFeO_3$ is prepared from starting materials about analytical purity, secondary phases next to $BiFeO_3$ can be formed, i.e. an orthorhombic $Bi_2Fe_4O_9$ mullite and a cubic $Bi_{25}FeO_{40}$ sillenite [28].

Problematics of antiferromagnetic behavior which is specific for $BiFeO_3$, can be also influenced by chemical doping. When substitution of Bi^{3+} is realized by ions with smaller ionic radius (especially by lanthanides) the magnetic anisotropy increases and the field required to cancel the magnetic cycloid reduces [29-31].

The multiferroic properties of the lanthanides-doped $BiFeO_3$ are discussed in many works, and only few researches devote interest to the investigation of chromaticity and another properties of these materials. According to the work of Yuan L. et al. [32] lanthanum-doped $BiFeO_3$ can serve as potential candidates for "cool pigments" due to their higher NIR reflectance. Therefore, based on these specific properties, these pigments could be used for applications as ceramic tiles or roofing material.

In this work, we concentrated on enhancement of the red colour in $PrFeO_3$ pigment. For this purpose, Bi^{3+} ion was chosen as a dopant. Therefore, the partial Bi substitution for Pr in $Bi_xPr_{1-x}FeO_3$ (x = 0-0.3) has been investigated with respect to their chromaticity and thermal stability. The compounds were prepared by conventional ceramic method. Moreover, the thermal behavior, particle size distribution and phase composition were also evaluated.

Experimental

Sample preparation

For preparation of all samples, Fe_2O_3 (99.6% purity, Precheza, a.s., Czech Republic), Bi_2O_3 (99.8 % purity, Lachema Pliva, a.s., Czech Republic) and Pr_6O_{11} (99% purity, importer-Trading Bochemie, s.r.o, Czech Republic) were used. Initial mixtures corresponding to chemical formula $Bi_xPr_{1-x}FeO_3$ (x = 0-0.3) were homogenized in a stoichiometric ratio in an agate mortar grinder Pulverisette 2 (Fritsch GmbH, Germany) for 20 min. Synthesis of all samples was performed with using classical ceramic route.

The each reaction mixture, which was an object of phase analysis control, was placed in a corundum crucible, inserted into a cold furnace and heated to the desired temperature. The calcination process was carried out at temperatures of 500-1000 °C with a step of 50 °C maintained for 1 min. The heating rate was 10 $°Cmin^{-1}$. The heat treatment intermediates were gradually cooled inside of the furnace to room temperature and after grinding in the agate mortar were subjected to XRD analysis for the determination of their phase composition.

To study the impact of partial Bi substitution on pigmentary properties of $Bi_xPr_{1-x}FeO_3$, the compounds were prepared by calcination process at 1000 °C and 1100 °C for a duration of 3 h. Heating rate of this calcination process was 10 °Cmin^{-1}.

The powder pigments were milled in order to improve their particle size distribution. Milling was carried out using a planetary mill Pulverisette 5 (Fritsch GmbH, Germany) in an ethanol and zircon beads (ϕ 1.1-1.2 mm). The following are the condition of milling: speed – 200 rpm, time of milling - 20 min and ball-to-powder mass ratio – 8:1.

Characterisation of samples

For the characterisation of thermal behaviour and formation of orthoferrites, the thermal analysis was carried out. Thermal analysis of the initial mixture for the synthesis of $Bi_{0.1}Pr_{0.9}FeO_3$ was performed using the STA 449C Jupiter (Netzsch, Germany), allowing the simultaneous registration of the thermoanalytical TG and DTA curves. The reaction mixture of approximately 360 mg was placed in a corundum crucible. Initial mixture was studied in the temperature region 20-1000 °C under following atmosphere: below 750 °C - air, above 750 °C – argon. The flow rate of the argon was 50 mL min^{-1}. The heating rate was 10 °Cmin^{-1}. α-Al_2O_3 (Sigma Aldrich, s r.o., Czech Republic) was used as the reference inert material [33].

The thermal stability of heat-treatment powders was verified by heating microscope EM201-12 (Hesse-Instr., Germany). Microscope is equipped with automatic image analysis. Tested samples compressed into tablets of 3 mm diameter and 6 mm high were heated from room temperature up to 1500 °C with a heating rate of 10°Cmin^{-1}. The changes in the area of the samples were observed.

The phase composition of all powder was analysed using a Miniflex 600 (Rigaku, Japan) diffractometer working in Bragg-Bretano geometry (Θ/2Θ) with 1D D/teX Ultra silicon strip detector an K_β filter. The Cu K_α radiation was used for this analysis. More precisely, Cu $K_{\alpha1}$ (λ=0.15418 nm) radiation was used for the range of 2Θ < 35°, and Cu $K_{\alpha2}$ (λ=0.15405 nm) was used for the range of 2Θ > 35°. The measurement conditions are as follows: scan range – 10° - 80°, step size – 0.02°, speed – 10°min^{-1}. The phase identification of studied powder was achieved with a program matching the diffraction patterns with data contained in the JCPDS database [34].

Particle size distribution was measured by Mastersizer 2000/MU (Malvern Isntruments, Ltd., UK). It is the highly integrated laser measuring system (He-Ne laser, λ=633 nm) intended for the analysis of particle size distribution. The laser passes through the dispersion media and is diffracted by the particles. The laser diffraction pattern was measured and the particle size distribution was evaluated based on Fraunhofer bending.

The main attention of this work focused on study of the influence of partial Bi substitution in $Bi_xPr_{1-x}FeO_3$ on colour properties of prepared orthoferrites. The colour properties of pigment powder and pigments applied into an organic acrylate matrix (Luxol, AkzoNobel, Czech Republic) into mass tone [18] were measured in the visible region of light (400-700 nm) using a ColourQuest XE (HunterLab, USA) spectrophotometer. The

measurement conditions of this assessment were following: an illuminat D65 (6500K); complementary observed - 10°; geometry of measurements – d/8°. The colour properties were described in the CIE$L^*a^*b^*$ system (1976), where the L^* represents the lightnes or darkness and it ranges from zero (black) to hundred (white). The values a^* (the axis red-green) and b^* (the axis yellow-blue) have a function of chromaticity showing the colour direction [35].

For better description of the colour, the next colour characteristics were calculated. The total colour differences ΔE^*_{CIE} is expressed by the formula $\Delta E^*_{CIE} = ((\Delta L^*)^2+(\Delta a^*)^2+(\Delta b^*)^2)^{1/2}$, where ΔL^* - brightness difference between a standard and a sample; Δa^*, Δb^* - difference of colour coordinates between a standard and a sample. The standard in our case $PrFeO_3$ and the sample with different Bi content ($Bi_xPr_{1-x}FeO_3$, where x = 0.1-0.3) were compared. The chroma C is calculated according to formula $C = (a^{*2}+b^{*2})^{1/2}$. It represents the saturation of the colour, and the C values are in the range 0-100 [18]. The colour hue of the pigments is possible to formulate as a hue angle $H° = arctg(b^*/a^*)$ [35]. The interval $H°$ for this studied system of pigments is as follows: 350°-35° red hue, 35°-70° orange hue.

Results and discussion

At the beginning, it is necessary to determine reactions taking place between the initial raw materials during heating at high temperatures. Therefore, an initial mixture corresponding to the theoretical formula $Bi_{0.1}Pr_{0.9}FeO_3$ was prepared. The evaluation of the thermal behaviour of this mixture was supported not only by the results of the X-ray diffraction analysis, but also based on our earlier results of TG/DTA analysis of the raw materials reported in the our previous works [36-39]. The TG and DTA thermoanalytical curves provide the information about reactions between chemical ingredients and formation of compound. Figure 1 shows TG/DTA curves of the initial mixture for the synthesis of $Bi_{0.1}Pr_{0.9}FeO_3$ which was performed in temperature region of 20-1000 °C. In this region, several endothermic effects were detected. The first one major endothermic effect with minimum at 354 °C and the following endothermic peak with minimum at 426 °C are connected with the reduction of Pr_6O_{11} (a dual oxide $4PrO_2 \cdot Pr_2O_3$) to the Pr_2O_3 [37] and successive losses of oxygen in the Pr_6O_{11} lattice. In the DTA curve, there is a slight decline indicating an endothermic effect at a temperature about 493 °C and it can be assigned to the phase transition of Fe_2O_3 from β into α - form [38,40,41]. Subsequent endothermic effect with minimum 644 °C corresponds not only to phase transformation of a monoclinic α-Bi_2O_3 to a cubic modification δ-Bi_2O_3 [36,39,42], but also to another partial reduction of praseodymium oxide [37,38,43]. In the DTA curve, there is a weak indication of an endothermic effect at a temperature of 713 °C and it can be interpreted as the start of solid solution formation of $Bi_xPr_{1-x}FeO_3$. This statement can be supported by the results of XRD analysis (Table 1, Fig. 2). XRD analysis proved that only starting materials were detected up to 650 °C in the initiation mixture. Diffraction lines corresponding to α-$BiFeO_3$ were first identified next to other reagents at 700 °C. Praseodymium ferrite oxide began to appear at 750 °C. A barely noticeable decrease indicating on the DTA curve an endothermic effect at a temperature of about 800 °C is connected with the phase transformation of α-$BiFeO_3$ on β-$BiFeO_3$ [28,44]. The last endothermic effect on the DTA curve is probably associated with

the peritectical decomposition of β-$BiFeO_3$ to $Bi_2Fe_4O_9$ and the amorphous (liquid) phase [26,44-45]. This outcome is in conformity with the results of XRD analysis, because the initial mixture annealed at 1000 °C did not contain $Bi_2Fe_4O_9$ phase [44].

Total mass loss detected in the TG curve was 5.57%. The first decrease in mass (0.89%) recorded on the TG curve at the temperature range of 20-200°C can be connected with the loss of moisture. Next decline of about 2.89% was at the temperature range of 200-450 °C. It is related to the reduction of Pr_6O_{11} and oxygen loss in the Pr_6O_{11} lattice. Another break in the TG curve (mass loss 1.07%) recorded in the temperature region of 550-725 °C is probably associated with a partial loss of oxygen in Pr_6O_{11} [37,38,43]. The last mass loss (0.75%) is associated with the decomposition of β-$BiFeO_3$ to $Bi_2Fe_4O_9$ and the amorphous phase, and it was recorded between 825 and 975 °C [44].

Conditions of synthesis significantly affect the sample structure. XRD patterns of samples calcined at 1000 and 1100 °C with a annealing time of 3 h are shown at Fig. 3. For the investigated samples, diffraction lines with the highest intensities were found at positions $2\Theta \approx 22.7°$, 25.5°, 32.0°, 32.4° and 32.6°. The same diffraction lines were found for the comparative sample $PrFeO_3$. Nevertheless, the diffraction lines corresponding to $BiFeO_3$ were found at positions $2\Theta \approx 22.2°$, 32.0°, 32.4° and 32.6°. The XRD analysis results of doped samples show an overlap of the diffraction lines assigned to $BiFeO_3$ and $PrFeO_3$. An enlargement of the lines 2Θ between 22° and 23° confirmed a profile of peaks with the Gaussian format. Superposition of the diffraction lines with the Gaussian profile indicated the formation of $Bi_xPr_{1-x}FeO_3$ solid solutions. Obtained results for Bi-doped samples showed that intensities of diffraction lines grew with increasing amount of Bi in $Bi_xPr_{1-x}FeO_3$ compounds. Comparison of the XRD patterns of samples calcined at 1000 °C and 1100 °C discovered that powder with lower intensities was prepared at 1100 °C. Generally, the XRD analysis proved the creation of $Bi_xPr_{1-x}FeO_3$ solid solutions. The mullite structure was not found in any sample.

Verification of the thermal stability of powder pigments is one of the other important pigmentary properties. Information about the dilatometric behaviour of the compounds during their heating is very significant. Based on these results, it is possible to choose a suitable ceramic glaze for study of the application properties of the tested powder. The thermal stability of prepared samples was studied using the heating microscope. The influence of partial Bi substitution for Pr on thermal stability of $PrFeO_3$ was determined. The thermal stability of all samples was verified in the temperature range of 25-1500 °C. A summary of results for all samples is given in Table 2. From the table, it is evident that there is a decreasing trend with increasing substitution. The dependence of area changes of powder prepared at 1000 °C on the heating temperature is shown in Fig. 4. Shape of the heating microscope curves pointed to decreasing thermal stability of pigments with increasing amount of Bi in $Bi_xPr_{1-x}FeO_3$ pigments. In addition, the shape of the curves, in particular for x = 0.2 and 0.3, showed that changes in the area of tablet took place in two stages. The first phase, which was found for all the measured powder, is associated with the start of sintering. However, the second phase, detected only for samples with higher content of Bi where pigment degradation was occurred, is probably associated with the melting of $BiFeO_3$. Deformation temperatures were determined at 1370 °C/1000 °C, 1356 °C/1100 °C for x = 0.2 and 1361 °C/1000 °C and 1325 °C/1100 °C for x =

0.3. Thermal stability of pure $BiFeO_3$ found by Dohnalová was limited at T_{def}=773 °C, and it was related to melting [39]. The higher thermal stability of orthoferrites in the present work compared to that in the literature may support the fact that Bi was introduced into $PrFeO_3$ and a solid solution was formed. The prepared pigments were thermally stable up to the temperature of 1200 °C, and therefore, for ceramic utilization, it is possible to recommend glazes with a glazing temperature of about 1150 °C.

For next application possibilities and assessment of the colour properties, it is necessary to know particle size distribution of the powder pigments. The mean particle size of about 2 μm is recommended for application into an organic binder. However, for this application, the d_{90} value is also very important, because it indicates on 90% representation of the particles in the system. If this parameter is large, it points out on the presence of coarse particles and it is necessary to improve the particle size distribution, the most often by milling. Obtained values of the particle size distribution of the prepared pigments are summarized in Table 3. The d_{50} values of the powder ranged from 1.52 to 3.57 μm for the samples calcined at 1000 °C and from 2.03 to 9.84 μm for the samples prepared at 1100 °C. The values of d_{90} were in range of 17-47 μm. Both the parameters determined for pigments crushed by hand in the agate mortar (marked before milling) pointed to the growth of coarse particles with increasing amount of Bi in $Bi_xPr_{1-x}FeO_3$. Moreover, the formation of coarse particles of the pigments with Bi was probably supported by their decreasing thermal stability associated with sintering. The measured values of particle size indicated an inappropriate particle size for the subsequent application of the pigments into the organic binder, so it was necessary to improve them by wet milling. Milling was carried out in the centrifugal planetary mill for 20 minutes using zircon beads under ethanol environment. A fine product was obtained, and the d_{90} was radically improved after 20 minutes. Even in the case of milled sample results, the slight growth of particle size with increasing substitution of bismuth in $Bi_xPr_{1-x}FeO_3$ compared with $PrFeO_3$ was well evident.

The main attention of this work was focused on the study of influence of partial Bi substitution on colour properties in $Bi_xPr_{1-x}FeO_3$ orthoferrites. Although results from the thermal analysis and phase composition indicated that the annealing temperature 1000 °C was sufficient for good reaction of the starting materials, the pigments were also prepared at 1100 °C. The reason was to follow a shift of the colouristic properties towards improvement or deterioration. The dependence of the partial Bi substitution on the colour a^*, b^* coordinates indicating the chromaticity of the $Bi_xPr_{1-x}FeO_3$ pigments is shown in Fig. 5. In this two-dimensional graph, the coordinate a^* was increased with the increasing content of Bi. This resulted in a growth of the red colour contribution compared to the original $PrFeO_3$. At the same time, the coordinate b^* was decreased and a loss of contribution of yellow colour was accompanied. Generally, the shift of colour from the orange area to the reddish orange was resulted.

This fact can be supported by other colour characteristics, which were obtained for powder and for the pigments after their application into the organic binder (Table 4 and 5). The colour hue of the all measured samples gradually decreased from the values typical for the pure orange shade to a value close to 35°, which is the limit for the transition of the orange colour to red. In conformity with Dohnalová et al., where authors discussed about the relationship of

orthoferrite colours and the ionic radius of lanthanides [18], $PrFeO_3$ can be described as yellowish brown (sienna) powder. In our case, positive shift of the colour from yellowish brown to reddish brown shades due to gradual substitution of Bi was recorded.

A darkening of samples with rising content of Bi was indicated by a decrease in the L^* coordinate towards lower values for all measured pigment sets. The direction of the moving of the a^*, b^* coordinates obtained for the powders was preserved even in the case of pigments applied into the organic binder. The colour saturation was decreased due to partial substitution, but this decline can be described as very small and insignificant. However, the values of total colour differences ΔE^*_{CIE} were large and proved that the changes in colour were significant. The ΔE^*_{CIE} values grew with increasing content of Bi in $Bi_xPr_{1-x}FeO_3$ pigments.

If all colour properties were compared, it was found that the calcination temperature of 1100 °C was not suitable for the preparation of the $Bi_xPr_{1-x}FeO_3$ type pigment. At this temperature, pigments with fundamentally lower values of a*, b* coordinates (when lower contribution of red and yellow colour was detected), with darker shades (lower L^* values), and decreasing saturations were prepared. These negative results were probably due to the melting of $BiFeO_3$.

Conclusion

In this work, the influence of partial Bi substitution on chromaticity and thermal stability of $Bi_xPr_{1-x}FeO_3$ pigments (x = 0-0.3) was investigated. The pigments were prepared by conventional ceramic method. The optimal temperature necessary for the formation of orthoferrites was determined by the thermal analysis method. The results of this study show that rising amount of Bi in $Bi_xPr_{1-x}FeO_3$ affected negatively their thermal stability, but substitution has a positive impact on the colour properties. The thermal stability of samples x = 0.2 and x = 0.3 was limited at 1371 °C, 1360 °C respectively, when deformation temperatures were detected. Deformation temperatures were associated with the melting of $BiFeO_3$. However, the partial Bi substitution for Pr significantly affected the colour of the original $PrFeO_3$. The colour of powders gradually shifted from yellowish brown ($PrFeO_3$) to reddish brown ($Bi_xPr_{1-x}FeO_3$, where x = 0.1-0.3) with the increase in the amount of Bi^{3+}. The coordinate a^* related to the red tone of the colour increased from 15.66 (x = 0) to 19.60 (x = 0.3) with rising substitution of Bi in $Bi_xPr_{1-x}FeO_3$. The saturation of the powder pigments has been enhanced by application in the organic binder. Increasing of calcination temperature to 1100 °C caused the creation of pigments with worse colour properties and with lower thermal stability. In view of the evaluation of a suitable quantity with respect to chromaticity and thermal stability, it is possible to recommend the amount of Bi of x = 0.2 for the preparation of $Bi_xPr_{1-x}FeO_3$ pigments and their application for ceramic glazes.

Acknowledgements

This work has been supported by Grant Agency of Czech Republic, Project No. 16-06697S.

References

1. Swiller DR. Inorganic Pigments. Kirk-Othmer Encyclopedia of Technol. 5th ed. New York: Wiley and sons; 2006.
2. Ahmed MA, El-Dek SI. Extraordinary role of Ca^{2+} ions on the magnetization of $LaFeO_3$ orthoferrite. Mater Sci Eng. 2006; B128:30-3.
3. Dohnalová Ž, Vontrončíková M, Šulcová P. Characterization of metal oxide-doped lutetium orthoferrite powders from the pigmentary point of view. J Therm Anal Calorim 2013;113:1223-9.
4. Geller S. Crystal structure of gadolinium orthoferrite, $GdFeO_3$. J Chem Phys. 1956; 24: 1236-9.
5. Cristóbal AA, Botta PM, Bercoff PG, Aglietti EF, Bertorello HR, Porto López JM. Mechanochemically assisted synthesis of yttrium-lanthanum orthoferrite: Structural and magnetic characterization. J Alloy Compd. 2010;495:516-9.
6. Minh NQ. Ceramic fuel cell. J Am ceram Soc. 199;79:563-88.
7. Shimizu Y, Shimabukuri M, Arai H, Seiyama T. Enhancement of humidity sensitivity for peroskite-type oxides having semiconductivity. Chem Lett. 1985; 917-20.
8. Obayashi H, Kudo T. Properties of oxygen deficient perovskite-type compounds and their use as alcohol sensors. Nippon Kagaku Kaishi. 1982; 1568-72.
9. Takahashi Y, Taguchi H. Effect of carbon monoxide oxidation on electrical properties of $(La_{0.8}Sr_{0.2})FeO_3$, J Mat Sci Lett. 1984;3:251-3.
10. Traversa E, Matsushima S, Okada Y, Sadaoka Y, Sakai Y, Watanabe K. NO_2 sensitive $LaFeO_3$ thin films prepared by R.F. sputtering. Sensors and Actuators B. 1995;25:661-4.
11. Arakawa T, Kurachi H, Shiokawa J. Physicochemical properties of rare earth perovskite oxide used as gas sensor material. J Mater Sci. 1985;4:1207-10.
12. Bouwmeester HJM, Kruidhof H, Burggraaf AJ. Importance of the surface exchange kinetics as rate limiting step in oxygen permeation through mixed-conducting oxides. Solid State Ionics. 1994;72:185-94.
13. Inoue T, Seki N, Egushi K, Arai H. Low-temperature operation of solid electrolyte oxygen sensors using perovskite-type oxide electrodes and cathodic reaction kinetics. J Electrochem Soc. 1990;137:2523-27.
14. Alcock CB, Doshi RC, Shen Y. Perovskite electrodes for sensors. Solid State Ionics.1992;51:281-9.
15. McCarty JG, Wise H. Perovskite catalysts for methane combustion. Catal Today.1990;8:231-48.
16. Tabata K, Misono M. Elimination of pollutant gases – oxidation of CO, reduction and decomposition of NO.1990;8:249-61.
17. Sreeram KJ, Aby CHP, Nair BU, Ramasami T. Colored cool colorants based on rare earth metal ions. Sol Energy Mater Sol Cells. 2008;92:1462-7.
18. Dohnalová Ž, Šulcová P., Trojan M. Synthesis and characterization of $LnFeO_3$ pigments. J Therm Anal Calorim. 2008;91:559-63.
19. Teague JR, Gerson R, James WJ. Dielectric hysteresis in single crystal $BiFeO_3$. Solid State Commun. 1970;8:1073-5.

20. Kubel F, Schmid H. Structure of a ferroelectric and ferroelastic monodomain crystal of the perovskite $BiFeO_3$. Acta Cryst B. 1990;46:698-702.
21. Lebeugle D, Colson D, Forget A, Viret M. Very large spontaneous electric polarization in $BiFeO_3$ single crystals at room temperature and its evolution under cycling fields. Appl Phys Lett. 2007;91:022997.
22. Kaczmarek W, Pająk Z, Połomska M. Differential thermal analysis of phase transition in $(Bi_{1-x}La_x)FeO_3$ solid solution. Solid State Commun. 1975;17:807-10.
23. Fischer W, Pająk Z, Połomska M. Differential thermal analysis of phase transition in $(Bi_{1-x}La_x)FeO_3$ solid solution. Solid State Commun. 1975;17:807-10.
24. Smolenskii GA, Chupis IE. Ferroelectromagnets. Sov Phys Usp. 1982;25:475-93.
25. Arnold DC, Knight KS, Catalan G, Redfern SAT, Scott JF, Lightfoot P, Morrison FD. The β-to-γ transition in $BiFeO_3$: a powder neutron diffraction study. Adv Funct Mater. 2010;20:2116-23
26. Palai R, Palai R, Kartiyar RS, Schmid H, Tissot P, Clark SJ, Robertson J, Redfern SAT, Catalan G, Scott JF. β phase and γ-β metal insulator transition in multiferroic $BiFeO_3$. Phys Rev B. 2008;77:014110.
27. Arnold DC, Knight KS, Morrison FD, Lightfoof P. Ferroelectric-paraelectric transition in $BiFeO_3$: crystal structure of the orthorhombic β phase. Phys Rev Lett. 2009;102:027602.
28. Valant M, Axelsson AK, Alford N. Peculiarities of a solid-state synthesis of multiferroic polycrystalline $BiFeO_3$. Chem Matt. 2007;19:5431-6.
29. Le Bras G, Colson D, Forget A, Genand-Riondet N, Tourbot R, Bonville P. Magnetization and magnetoelectric effect in $Bi_{1-x}La_xFeO_3$ ($0 \leq x \leq 0.15$). Phys Rev B. 2009;80:134417.
30. Chen P, Günaydın-Şen Ö, Ren JW, Qin Z, Brinzari TV, McGill S, Cheong SW, Musfeldt JL. Spin cycloid quenching in Nd^{3+} -substituted $BiFeO_3$. Phys Rev B. 2012;83:014407.
31. Khomchenko VA, Paixão JA. Ti doping-induced magnetic and morphological transformations in Sr- and Ca-substituted $BiFeO_3$. J Phys: Condens Matter. 2016;28:166004.
32. Yuan L, Han A, Ye M, Chen X, Yao L, Ding Ch. Synthesis and characterization of environmentally benign inorganic pigments with high NIR reflectance: Lanthanum-doped $BiFeO_3$. Dyes and Pigm. 2018;148:137-46.
33. Pelovski Y, Petkova V, Dombalov I. Thermotribochemical treatment of low grade natural phosphates. J Therm Anal Calorim. 2007;88:207-12.
34. Joint Committee on Powder Diffraction Standards. International centre of diffraction data. Swarthmore: JCPDS; 1983.
35. Commission Internationale de l´Eclairage. Recommendations on uniform colour space, colour difference equations, psychometric colopur terms. Supplement No 2 of CIE publication no 15 (E1-1,31) 1971, Paris Bureau Central de la CIE; 1978.
36. Šulcová P, Trojan M. Thermal analysis of pigments based on Bi_2O_3. J Therm Anal Calorim. 2006;84:737-40.
37. Šulcová P, Trojan M. Study of $Ce_{1-x}Pr_xO_2$ pigments. Thermochim Acta. 2003;395:251-5.

38. Luxová J, Šulcová P, Trojan M. Influence of firing temperature on the color properties of orthoferrite $PrFeO_3$. Thermochim Acta. 2014;579:80-5.
39. Dohnalová Ž, Šulcová P, Bělina P, Vlček M, Gorodylova N. Brown pigments based on perovskite structure of $BiFeO_{3-\delta}$. J Therm Anal Calorim. 2018;133:421-8.
40. Zbořil R, Mashlan M, Krausova D, Pikal P. Cubic β-Fe_2O_3 as the product of the thermal decomposition of $Fe_2(SO_4)_3$. Hyperfine Interact. 1999;120:497-501.
41. Danno T, Asaoka H, Nakanishi M, Fujii T, Ikeda Y, Kusano, Y, Takada J. Formation mechanism of nano-crystalline β-Fe_2O_3 particles with bixbyite structure and their magnetic properties. J Phys: Conf Ser. 2010;200:082003.
42. Polat Y, Mehmet A, Dağdemir Y. Magnetic properties of Co-doped Bismuth oxide (δ-Bi_2O_3) at low temperature. J Low Temp Phys. 2018;193:74-84.
43. Abdellahi M, Abhari AS, Bahmanpour M. Preparation a characterization of orthoferrite $PrFeO_3$ nanoceramic. Ceram Int. 2016;42:4637-41.
44. Maître A, François M, Gachon JC. Experimental study of the Bi_2O_3-Fe_2O_3 pseudo-binary system. J Phase Equilib Diffus. 2004;25:59-67.
45. Selbach SM, Einarsrud MA, Grande T. On the thermodynamic stability of $BiFeO_3$. Chem Mater. 2009;21:169-73.

Figure caption

Fig. 1

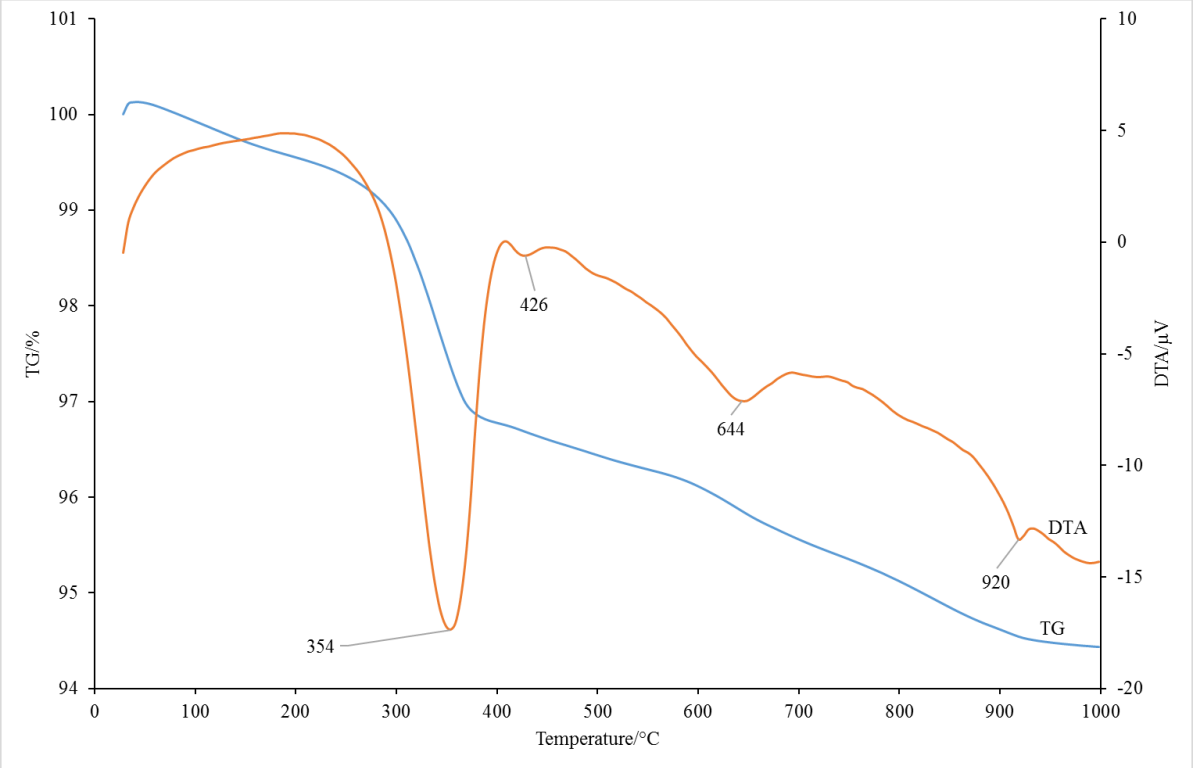

Fig. 2

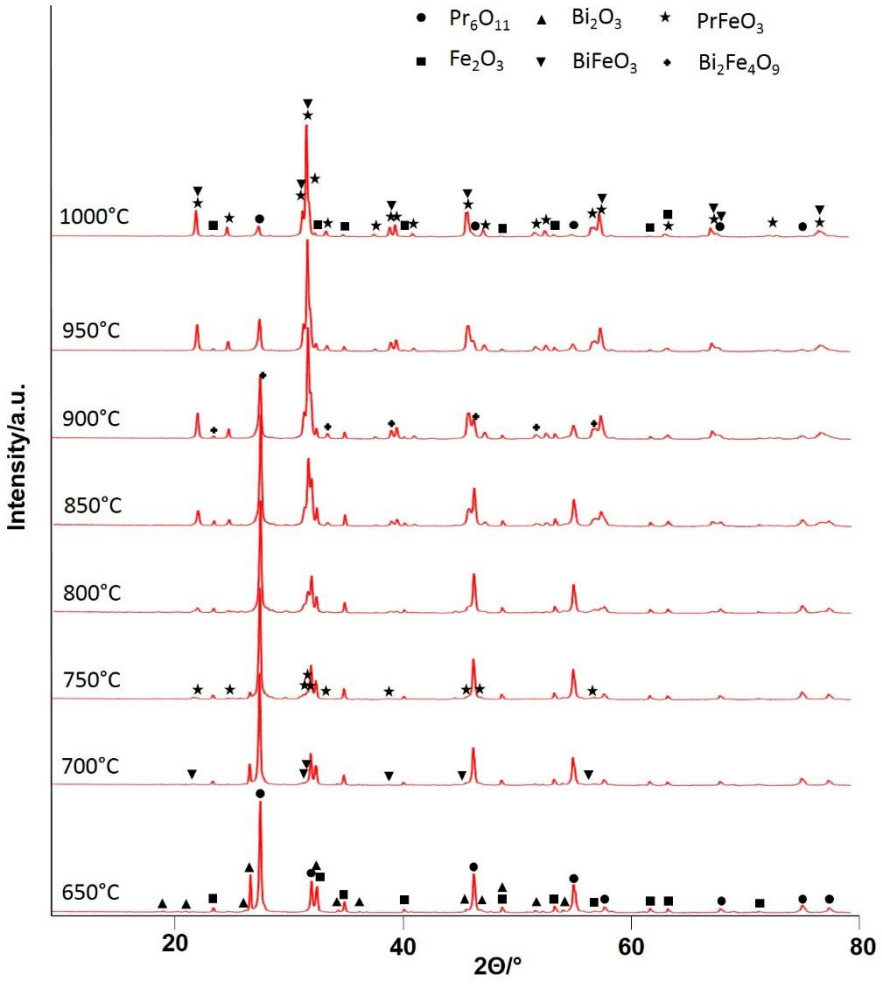
Pr6O11
Bi2O3
PrFeO3
Fe2O3
BiFeO3
Bi2Fe4O9
1000°C
950°C
900°C
850°C
800°C
750°C
700°C
650°C
Intensity/a.u.
20
40
60
80
2Θ/°

Fig. 3a

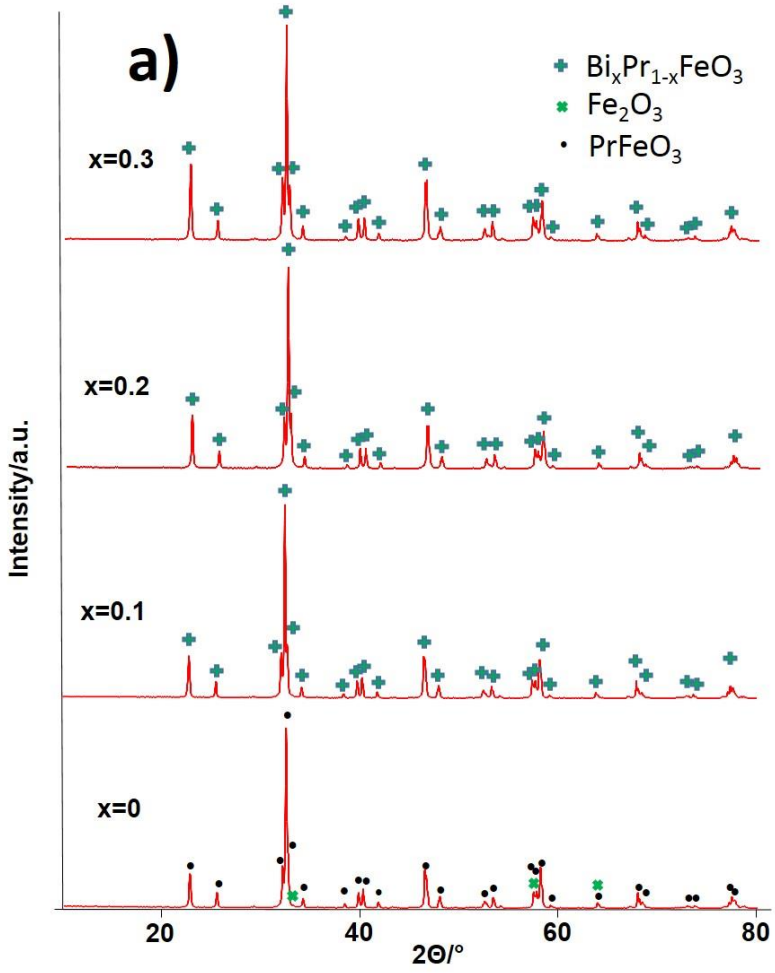
a)
$Bi_xPr_{1-x}FeO_3$
Fe_2O_3
$PrFeO_3$
x=0.3
x=0.2
x=0.1
x=0
Intensity/a.u.
20
40
60
80
2Θ/°

Fig 3b

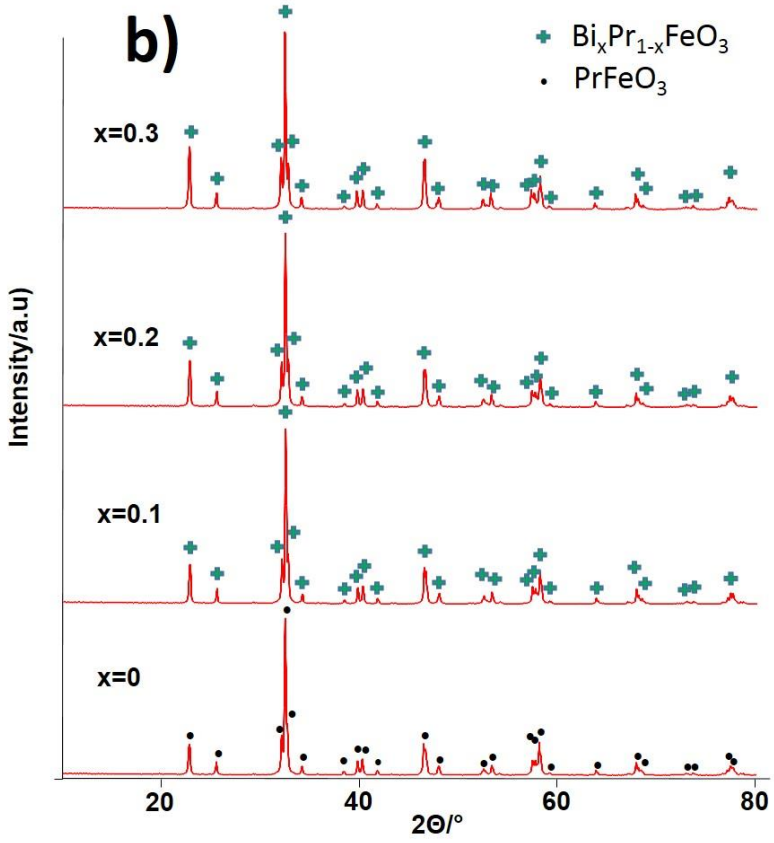
b)
$Bi_xPr_{1-x}FeO_3$
$PrFeO_3$
x=0.3
x=0.2
x=0.1
x=0
Intensity/a.u)
20
40
60
80
2Θ/°

Fig. 4

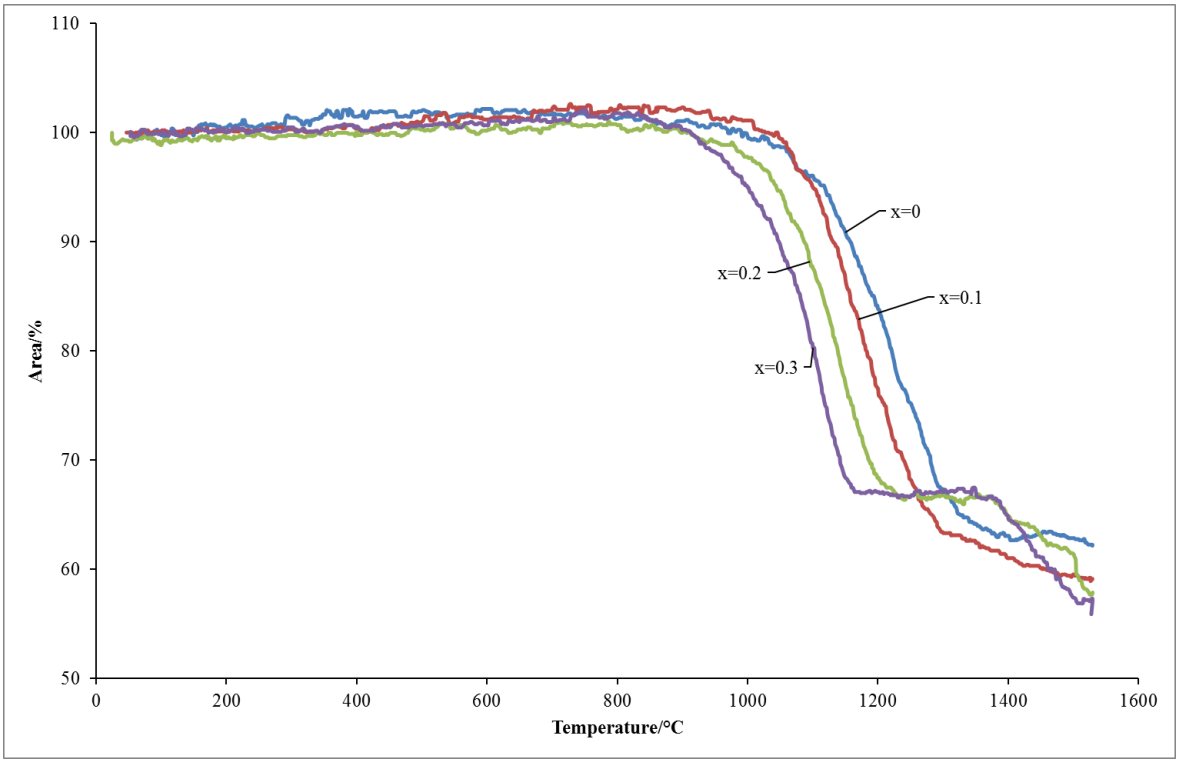
110
100
90
80
70
60
50
Area/%
0
200
400
600
800
1000
1200
1400
1600
Temperature/°C
x=0
x=0.2
x=0.1
x=0.3

Fig. 5

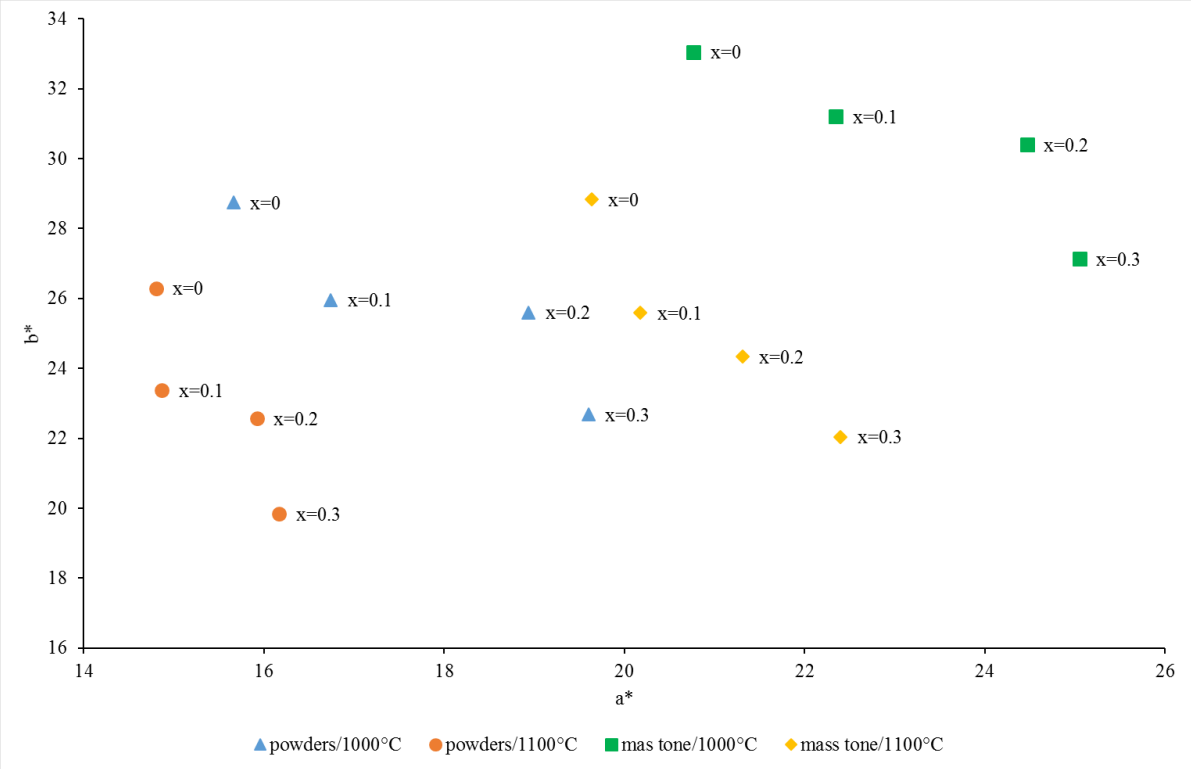
34
32
30
28
26
24
22
20
18
16
b*
14
16
18
20
22
24
26
a*
x=0
x=0.1
x=0.2
x=0.3
x=0
x=0
x=0.3
x=0
x=0.1
x=0.2
x=0.1
x=0.2
x=0.1
x=0.2
x=0.3
x=0.3
x=0.3
powders/1000°C
powders/1100°C
mas tone/1000°C
mass tone/1100°C

Tables

Table 1

Tempetarure/°C	Identified Phase
500	Pr_6O_{11}, β-Fe_2O_3, α-Fe_2O_3, α-Bi_2O_3
550	Pr_6O_{11}, β-Fe_2O_3, α-Fe_2O_3, α-Bi_2O_3
600	Pr_6O_{11}, β-Fe_2O_3, α-Fe_2O_3, α-Bi_2O_3
650	Pr_6O_{11}, α-Fe_2O_3, β-Fe_2O_3, δ-Bi_2O_3
700	Pr_6O_{11}, α-Fe_2O_3, δ-Bi_2O_3, α-$BiFeO_3$
750	Pr_6O_{11}, α-Fe_2O_3, $PrFeO_3$, δ-Bi_2O_3, α-$BiFeO_3$
800	Pr_6O_{11}, α-Fe_2O_3, $PrFeO_3$, α-$BiFeO_3$, β-$BiFeO_3$
850	Pr_6O_{11}, $PrFeO_3$, β-$BiFeO_3$, α-Fe_2O_3
900	$PrFeO_3$, β-$BiFeO_3$, Pr_6O_{11}, α-Fe_2O_3, $Bi_2Fe_4O_9$
950	$PrFeO_3$, β-$BiFeO_3$, Pr_6O_{11}, α-Fe_2O_3, $Bi_2Fe_4O_9$
1000	$PrFeO_3$, β-$BiFeO_3$, Pr_6O_{11}, α-Fe_2O_3

Table 2

x	1000 °C		1100 °C	
	$T_{sintr.}$/°C	$T_{def.}$/°C	$T_{sintr.}$/°C	$T_{def.}$/°C
0	1086	-	1062	-
0.1	1059	-	1047	-
0.2	1019	1370	976	1356
0.3	996	1361	956	1325

$T_{sintr.}$ start of sintering temperature/°C; $T_{def.}$ deformation temperature/°C

Table 3

x	Before milling				After milling			
	1000 °C		1100 °C		1000 °C		1100 °C	
	d_{50}/μm	d_{10}-d_{90}/μm	d_{50}/μm	d_{10}-d_{90}/μm	d_{50}/μm	d_{10}-d_{90}/μm	d_{50}/μm	d_{10}-d_{90}/μm
0	1.52	0.48-17.21	2.03	0.83-23.95	0.92	0.37-2.11	1.08	0.40-2.88
0.1	1.69	0.57-27.83	2.41	0.52-20.64	0.91	0.35-2.16	1.25	0.33-3.40
0.2	2.08	0.61-34.16	6.63	1.06-23.81	0.91	0.35-2.22	1.28	0.31-3.55
0.3	3.57	0.67-46.85	9.84	1.25-35.97	0.99	0.36-2.64	1.59	0.33-4.33

Table 4

x	1000 °C				1100 °C			
	L*	C	H°/°	ΔE^*_{CIE}	L*	C	H°/°	ΔE^*_{CIE}
0	59.10	32.74	61.42	-	57.21	30.17	60.12	-
0.1	57.23	30.89	57.19	3.53	56.10	27.70	57.54	3.15
0.2	56.16	31.84	53.51	5.41	55.18	27.62	54.80	4.41
0.3	54.92	29.98	49.17	8.36	54.56	25.60	50.82	7.13

Table 5

x	1000 °C				1100 °C			
	L*	C	H°/°	ΔE^*_{CIE}	L*	C	H°/°	ΔE^*_{CIE}
0	48.98	39.03	57.85	-	46.44	34.88	55.74	-
0.1	47.61	38.38	54.38	2.79	44.10	32.59	51.74	4.03
0.2	47.03	39.02	51.17	4.93	43.67	32.35	48.80	5.53
0.3	44.83	36.92	47.28	8.40	42.72	31.42	44.54	8.22

List of figures:

List of tables: